Δ self-energy at finite temperature and density and the πN cross-section

Snigdha Ghosh, Sukanya Mitra and Sourav Sarkar

Theoretical High Energy Physics Division, Variable Energy Cyclotron Centre

1/AF Bidhannagar, Kolkata - 700064

arXiv:1603.06699v1 [hep-ph] 22 Mar 2016

Abstract

The self energy of Δ-baryon is evaluated at finite temperature and density using the real time formalism of thermal field theory. The Dyson-Schwinger equation is used to get the exact thermal propagator followed by the spectral function of Δ. The πN scattering cross section obtained using explicit Δ exchange is normalized to the experimental data in vacuum and its medium modification is implemented by means of the exact thermal propagator. A significant suppression of the peak is observed at higher temperature and baryon density.

I. INTRODUCTION

The properties of hadrons under conditions of high temperature and/or baryon density have been widely studied owing to the possibility of restoration of chiral symmetry of QCD spontaneously broken by the vacuum [1]. Relativistic collisions of heavy ions provide the unique opportunity to actually produce hot/dense matter under controlled conditions and provide experimental verification of such studies(see e.g. [2]). The broadening of vector spectral function in the medium observed through the invariant mass spectra of dileptons in heavy ion collisions at SPS [3] and RHIC has been interpreted to have non-trivial, though indirect implications on chiral symmetry restoration [4].

Cross-sections of scattering between excitations in the medium could be non-trivially affected by the presence of other particles constituting it. The case of the $\pi\pi$ cross-section in a hot pion gas was studied by Barz et al [5] obtaining a substantial reduction of the magnitude in the region of the ρ peak. In addition to the usual quantum fluctuations, thermal fluctuations modify the propagation of mediating particles and consequently the invariant amplitude. Recently [6], the amplitudes for elastic $\pi\pi$ scattering were evaluated using in-medium propagators for the exchanged ρ and σ mesons incorporating loop graphs with π, ω, h_1 and a_1 mesons in the internal lines [7]. The in-medium cross-section so obtained showed a substantial reduction in magnitude at the peak position. When used in the collision integral of the transport equation, these medium modified scattering amplitudes were found to significantly affect the transport properties of a hot pion gas [8, 9].

In this work we study the πN cross-section in a hot and dense gas consisting of pions and nucleons. We concentrate in the centre of mass energy region of the lightest baryon resonance, the Δ, which is close to an ideally elastic πN resonance, decaying almost entirely into π and N. Despite being relatively broad, it is well separated from other resonances. We evaluate one-loop self-energies with π, ρ, N and Δ in the internal lines using standard thermal field theoretic methods. The in-medium propagator of the Δ is then used in the scattering amplitudes to obtain the πN cross-section. Medium modifications of the Δ resonance has been studied mostly in nuclear matter [10–14] and a few at finite temperature [15, 16]. Also, properties of the Δ have been studied experimentally using invariant mass analyses of πN pairs [17, 18].

In the next section we recall some basic features of the real-time version of thermal field

theory. Then we evaluate the Δ self-energy and discuss numerical results. In the following section we evaluate the amplitudes of πN scattering and finally the cross-section in the medium. This is followed by summary and discussions. Some details of the calculation is provided in the Appendix.

II. THE Δ SELF-ENERGY IN THE MEDIUM

A. The in-medium propagators in the real time formalism

In the real time formalism of thermal field theory, all two-point functions including the self-energy take the form of 2×2 matrices [19, 20]. But each of the matrices may be diagonalized, when it is given essentially by a single analytic function which determines completely the dynamics of the corresponding two-point function. This function being given by any one, say the 11-component of the matrix, we need to evaluate only this component of the self-energy matrix. In the following we specify only the 11-component of the thermal propagator for the particles involved in the one-loop graphs that are considered in this work.

The 11-component of a free thermal propagator matrix for a particle consists of its vacuum propagator and a term depending on the on-shell distribution function of like particles in the medium through which it propagates. The form of the latter term depends only on whether the particle in question is a boson or a fermion. The 11-component of the thermal pion propagator is given by

$$D_{11}(k, m_\pi) = \Delta(k, m_\pi) + 2\pi i N_1^2(k, m_\pi)\delta(k^2 - m_\pi^2) \tag{1}$$

where

$$\begin{aligned} \Delta(k, m) &= \frac{-1}{k^2 - m^2 + i\eta} \\ N_1(k, m) &= \sqrt{n_+^k}\Theta(k^0) + \sqrt{n_-^k}\Theta(-k^0) \end{aligned} \tag{2}$$

with

$$n_\pm^k = \frac{1}{e^{\beta(\omega_k \mp \mu_k)} - 1} \;\; ; \;\; \omega_k = \sqrt{\vec{k}^2 + m^2} \; .$$

The thermal part remaining same, the ρ propagator with the familiar polarization sum follows as

$$D_{11}^{\mu\nu}(k, m_\rho) = \left(-g^{\mu\nu} + \frac{k^\mu k^\nu}{m_\rho^2}\right) D_{11}(k, m_\rho) \; . \tag{3}$$

We now consider the fermionic propagators whose thermal (matrix) parts are different from the bosonic ones discussed above. The 11-components of the nucleon and Δ propagators are respectively given by

$$S^{11}(p) = (\not{p} + m_N)E^{11}(p, m_N) \tag{4}$$

and

$$S^{11}_{\mu\nu}(p) = (\not{p} + m_\Delta) \quad \left\{-g_{\mu\nu} + \frac{2}{3m^2_\Delta}p_\mu p_\nu + \frac{1}{3}\gamma_\mu\gamma_\nu \right. \\ \left. \frac{1}{3m_\Delta}(\gamma_\mu p_\nu - \gamma_\nu p_\mu)\right\} E^{11}(p, m_\Delta) \tag{5}$$

where, we recall from Appendix-A,

$$E_{11}(p, m) = \Delta(p, m) - 2\pi i\tilde{N}^2_1(p, m))\delta(p^2 - m^2) \tag{6}$$

with

$$\tilde{N}_1(p, m) = \sqrt{\tilde{n}^p_+}\theta(p^0) + \sqrt{\tilde{n}^p_-}\theta(-p^0);$$
$$\tilde{n}^p_\pm = \frac{1}{e^{\beta(\omega_p \mp \mu_p)} + 1}\ , \quad \omega_p = \sqrt{\vec{p}^2 + m^2}\ .$$

The complete propagator $\boldsymbol{S'}$ is given by the Dyson equation in terms of the free fermion propagator $\boldsymbol{S}$ and self-energy $\boldsymbol{\Pi}$,

$$\boldsymbol{S'} = \boldsymbol{S} + \boldsymbol{S}\,\boldsymbol{\Pi}\,\boldsymbol{S'} \tag{7}$$

where each is a 2×2 matrix in the thermal indices. They can be diagonalized to get the respective analytic functions, denoted by bar, so that

$$\overline{S}' = \overline{S} + \overline{S}\,\overline{\Pi}\,\overline{S}'\ . \tag{8}$$

The self-energy function $\overline{\Pi}$ can be obtained from any single component of the self energy matrix. As discussed in Appendix-A, it is related to the 11-component by

$$\begin{aligned} \mathrm{Im}\bar{\Pi}(p) &= \epsilon(p_0)\coth[\beta(p_0 - \mu_p)/2]\mathrm{Im}\Pi_{11}(p) \\ \mathrm{Re}\bar{\Pi}(p) &= \mathrm{Re}\Pi_{11}(p)\ . \end{aligned} \tag{9}$$

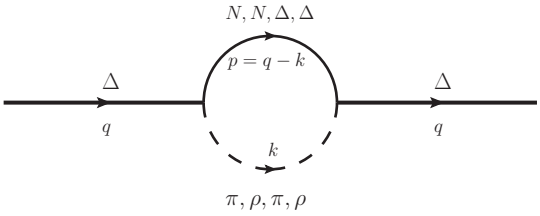

FIG. 1: Feynman Diagrams for Δ-Self Energy

B. The Δ self-energy

We begin by writing down the expressions for the one-loop self-energy graphs for the Δ *in vaccum*. For the four cases shown in fig. 1 they can be generally expressed as

$$\Pi^{\mu\nu}_{vac}(q) = i \int \frac{d^4k}{(2\pi)^4} N^{\mu\nu} \Delta(p) \Delta(k) \tag{10}$$

where $N^{\mu\nu}$ contains terms coming from the two vertices and the spin factors appearing in the propagators for the internal lines. They can be read off from the expressions for $\Pi^{\mu\nu}$ given in Appendix-B and appear as

$$N^{\mu\nu}_{\pi N\Delta} = \frac{f^2_{\pi N\Delta}}{m^2_\pi} F^2(p,k) \left[k_\alpha k_\beta \mathcal{O}^{\nu\beta} (\not{p} + m_p) \mathcal{O}^{\alpha\mu} \right] \tag{11}$$

$$N^{\mu\nu}_{\rho N\Delta} = \frac{f^2_{\rho N\Delta}}{m^2_\rho} F^2(p,k) \left[\mathcal{O}^{\nu\eta} \gamma^5 \left(\gamma_\beta k_\eta - g_{\beta\eta} \not{k} \right) \left(\not{p} + m_p \right) \gamma^5 \left(\gamma_\alpha k_\sigma - g_{\alpha\sigma} \not{k} \right) \mathcal{O}^{\mu\sigma} A_{\alpha\beta} \right] \tag{12}$$

$$N^{\mu\nu}_{\pi\Delta\Delta} = \frac{f^2_{\pi\Delta\Delta}}{m^2_\pi} F^2(p,k) \left[g_{\chi\psi} g_{\eta\phi} \mathcal{O}^{\nu\chi} \gamma^5 \not{k} \mathcal{O}^{\psi\sigma} \Sigma_{\lambda\sigma}(p) \mathcal{O}^{\lambda\eta} \gamma^5 \not{k} \mathcal{O}^{\phi\mu} \right] \tag{13}$$

$$\begin{aligned} N^{\mu\nu}_{\rho\Delta\Delta} = f^2_{\rho\Delta\Delta} F^2(p,k) \Bigg[& g_{\chi\psi} g_{\eta\phi} \mathcal{O}^{\nu\chi} \left(\gamma^\beta + i \frac{\kappa_{\rho\Delta\Delta}}{2m_\Delta} \sigma^{\beta\epsilon} k_\epsilon \right) \mathcal{O}^{\psi\theta} \Sigma_{\lambda\theta}(p) \\ & \mathcal{O}^{\lambda\eta} \left(\gamma^\alpha - i \frac{\kappa_{\rho\Delta\Delta}}{2m_\Delta} \sigma^{\alpha\delta} k_\delta \right) \mathcal{O}^{\phi\mu} A_{\alpha\beta} \Bigg] \end{aligned} \tag{14}$$

where

$$\begin{aligned} A_{\alpha\beta}(k) &= -g_{\alpha\beta} + \frac{k_\alpha k_\beta}{m^2_k} \quad \text{and} \\ \Sigma_{\alpha\beta}(q) &= (\not{q} + m_q) \left[-g_{\alpha\beta} + \frac{1}{3m^2_q} q_\alpha q_\beta + \frac{1}{3} \gamma_\alpha \gamma_\beta + \frac{1}{3m_q} \left(\gamma_\alpha q_\beta - \gamma_\beta q_\alpha \right) \right] . \end{aligned} \tag{15}$$

We now proceed to write down the corresponding expressions *in the medium*. As discussed above, we need to evaluate only the 11-component $\Pi^{\mu\nu}_{11}$ which is obtained by replacing the

vacuum propagators by the 11-component of thermal propagators given in the previous section. The self-energy in the medium is thus given by

$$\Pi_{11}^{\mu\nu}(q) = i \int \frac{d^4k}{(2\pi)^4} N^{\mu\nu} E_{11}(p) D_{11}(k) \ . \tag{16}$$

Expanding D_{11} and E_{11} we obtain in addition to $\Pi_{vac}^{\mu\nu}$, two terms which are linear in the thermal distribution function and the fourth term non-linear in the distribution function which is purely imaginary. Performing the k^0 integral and using eqns. (9) we obtain the imaginary and real parts of the self-energy function as

$$\begin{aligned} \mathrm{Im}\bar{\Pi}^{\mu\nu} = \quad & -\pi\epsilon(q_0) \int \frac{d^3k}{(2\pi)^3} \frac{1}{4\omega_k\omega_p} \\ & [N^{\mu\nu}(k^0=\omega_k)\{(1+n_+^k-\tilde{n}_+^p)\delta(q_0-\omega_k-\omega_p)+(-n_+^k-\tilde{n}_-^p)\delta(q_0-\omega_k+\omega_p)\} \\ & N^{\mu\nu}(k^0=-\omega_k)\{(-1-n_-^k+\tilde{n}_-^p)\delta(q_0+\omega_k+\omega_p)+(n_-^k+\tilde{n}_+^p)\delta(q_0+\omega_k-\omega_p)\}] \end{aligned} \tag{17}$$

and

$$\begin{aligned} \mathrm{Re}\bar{\Pi}^{\mu\nu} = \int \frac{d^3k}{(2\pi)^3} \frac{1}{2\omega_k\omega_p} \mathcal{P} \quad & \left[\left(\frac{n_+^k N^{\mu\nu}(k^0=\omega_k)}{(q_0-\omega_k)^2-\omega_p^2}\right)+\left(\frac{n_-^k N^{\mu\nu}(k^0=-\omega_k)}{(q_0+\omega_k)^2-\omega_p^2}\right)- \right. \\ & \left.\left(\frac{\tilde{n}_+^p N^{\mu\nu}(k^0=q_0-\omega_p)}{(q_0-\omega_p)^2-\omega_k^2}\right)-\left(\frac{\tilde{n}_-^p N^{\mu\nu}(k^0=q_0+\omega_p)}{(q_0+\omega_p)^2-\omega_k^2}\right)\right] \end{aligned} \tag{18}$$

where $\omega_k = \sqrt{m_k^2+\vec{k}^2}$ and $\omega_p = \sqrt{m_p^2+(\vec{q}-\vec{k})^2}$.

Each of the terms in the imaginary part can be related to scattering and decay of the Δ-baryon. The delta functions in the four terms define the kinematic domains where these processes occur. The regions where these are non-vanishing gives rise to branch cuts in the complex q_0 plane. The first and third terms in (17) are non-vanishing for $q^2 > (m_k+m_p)^2$. This is the unitary cut. The second and fourth terms which are non-zero for $q^2 < (m_p-m_k)^2$ defines the Landau cut and is purely a medium effect. Confining ourselves to the kinematic region $q_0 > 0$ and $q^2 > 0$, the first and fourth terms only contribute. The first corresponds to absorption of the Δ due to decay into a baryon-meson pair such as $N\pi$, $N\rho$ etc. and is thus weighted by a thermal factor $1+n_+^k-\tilde{n}_+^p = (1+n_+^k)(1-\tilde{n}_+^p)+n_+^k\tilde{n}_+^p$, indicating Bose enhancement of the meson and Pauli blocking of the baryon in the process $\Delta \to \pi N$ plus the usual thermal factors for the initial state in the time reversed process where the Δ is produced. The fourth term is due to absorption of the Δ due to scattering from a meson

producing a baryon in the final state and vice versa as is evident from the thermal weight factor $n_-^k + \tilde{n}_+^p = n_-^k(1-\tilde{n}_+^p) + \tilde{n}_+^p(1+n_-^k)$.

To take into account the finite width of unstable particles in the loop graphs the self-energy is folded with their spectral functions. For unstable mesons (h) we use [21],

$$\Pi(q,m_h) = \frac{1}{N_h}\int_{(m_h-2\Gamma_h)^2}^{(m_h+2\Gamma_h)^2} dM^2 \frac{1}{\pi}\mathrm{Im}\left[\frac{1}{M^2-m_h^2+iM\Gamma_h(M)}\right]\Pi(q,M) \tag{19}$$

with $N_h = \displaystyle\int_{(m_h-2\Gamma_h)^2}^{(m_h+2\Gamma_h)^2} dM^2 \frac{1}{\pi}\mathrm{Im}\left[\frac{1}{M^2-m_h^2+iM\Gamma_h(M)}\right]$.

For baryons (R) with non-trivial decay width in the loops we use

$$\Pi(q,m_R) = \frac{1}{N_R}\int_{m_R-2\Gamma_R}^{m_R+2\Gamma_R} dM \frac{1}{\pi}\mathrm{Im}\left[\frac{1}{M-m_R+\frac{i}{2}\Gamma_R(M)}\right]\Pi(q,M) \tag{20}$$

with $N_R = \displaystyle\int_{m_R-2\Gamma_R}^{m_R+2\Gamma_R} dM \frac{1}{\pi}\mathrm{Im}\left[\frac{1}{M-m_R+\frac{i}{2}\Gamma_R(M)}\right]$. This has the effect that the sharp thresholds of the branch cuts get smeared.

C. Numerical results

Let us begin with the results for the Δ self-energy in the medium. We show numerical results for the spin-averaged real and imaginary parts of the function Π given by [11, 13]

$$\Pi = \frac{1}{4}\sum_{s_\Delta} \bar{\Psi}_\mu \bar{\Pi}^{\mu\nu}\Psi_\nu \tag{21}$$

where $\bar{\Psi}_\mu$ denote Rarita-Schwinger spinors. The factors $N^{\mu\nu}$ given in eqs. (14) then go over to $\frac{1}{4}\mathrm{Tr}[N^{\mu\nu}\Sigma_{\mu\nu}]$. In fig. 2 we plot the Landau cut contribution to the imaginary part coming from the different loop graphs at $T = 100$ MeV for $\mu_N = 200$ MeV in the left panel and $\mu_N = 500$ MeV on the right. As discussed in the last section, it follows that for $\vec{q} = 0$ the Landau cut extends up to the difference of masses of the baryon and the meson in the loop graph in the stable limit. These contributions at lower values of q_0 are a result of scattering processes in the thermal medium and will be absent in vacuum. Comparing the left and right panels we see that the ρN and $\rho\Delta$ loops start contributing to the imaginary part only at larger baryon densities. At higher temperature, T=150 MeV the magnitudes become larger as seen in fig. 3. Though the πN loop dominates, significant contributions also come from the other loops.

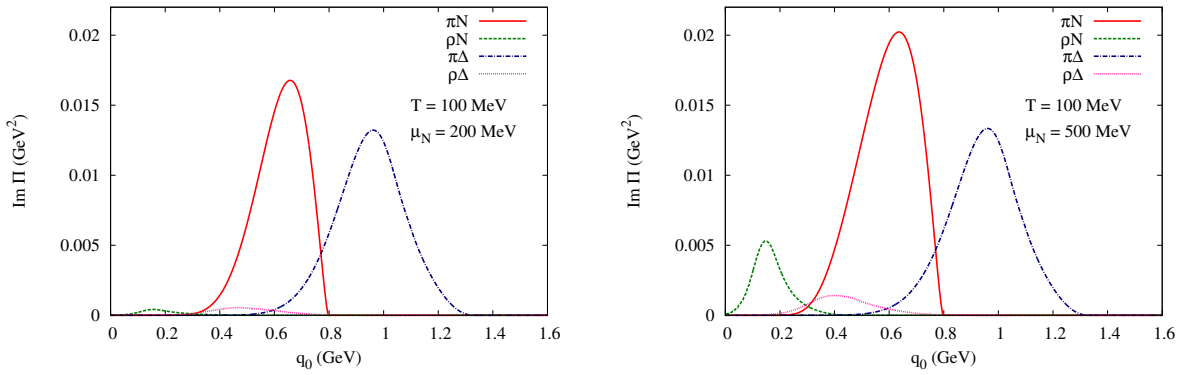

FIG. 2: The Landau-cut contribution to the imaginary part of the self energy function at T=100 MeV.

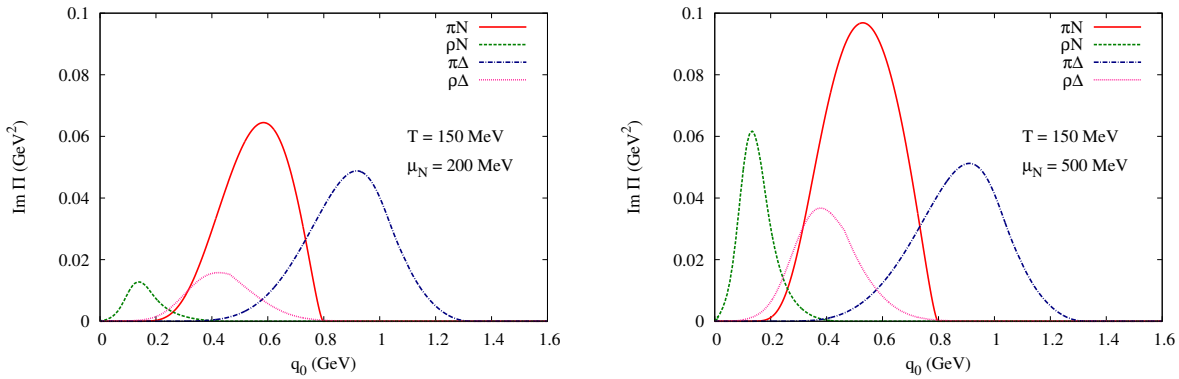

FIG. 3: Same as fig. 2 at T=150 MeV.

The unitary cut contributions to the imaginary part are much larger in magnitude than the ones coming from the Landau cut. The thresholds lie at higher energies, for stable particles starting from the sum of the nominal masses of the particles in the loop graph. Shown in fig. 4 are the unitary cut contributions from the four loops at $T = 100$ MeV. We observe the sequential opening up of heavier decay channels. These are the same as in vacuum but are now weighted by the Pauli blocking and Bose enhancement factors in the final state. The form factor suppresses the usual monotonous rise of these contributions at higher q_0.

We now consider the thermal component of the real part of the self-energy consisting of principal value integrals. As seen in figs. 5 and 6 the magnitudes are quite small compared to the imaginary parts and are not expected to contribute to a thermal shift in the pole position of the Δ.

Having obtained the imaginary and real parts of the self-energy we now plot the spectral

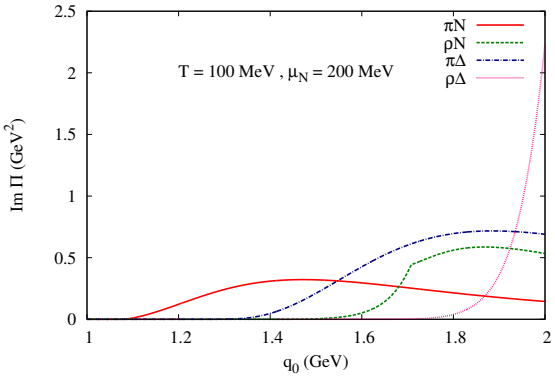

FIG. 4: The unitary cut contribution at T=100 MeV.

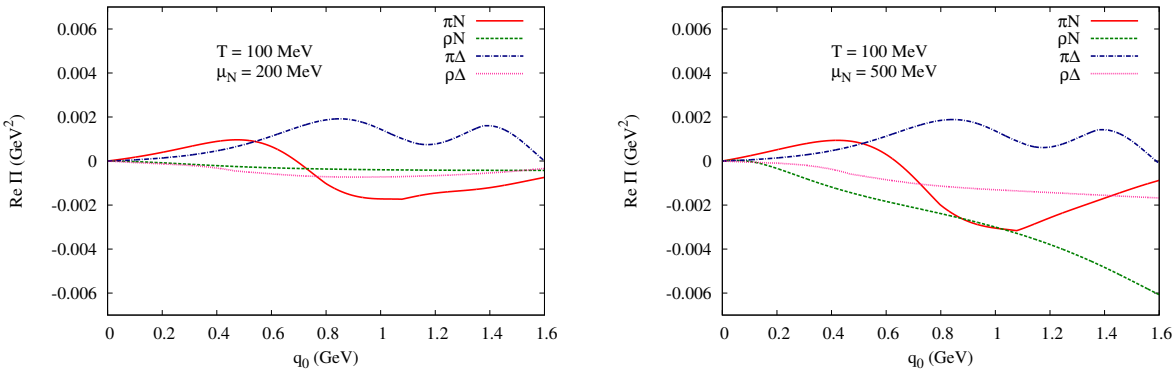

FIG. 5: The real part of the self energy function at T=100 MeV.

function which is the imaginary part of the complete propagator (8). We do so in two parts. The low q_0 region depicting the Landau cut contribution shown in the left panel of fig. 7 is purely a thermal contribution. The high q_0 region in the vicinity of the bare Δ mass consisting of the contributions from the unitary cuts is shown on the right of fig. 7. The

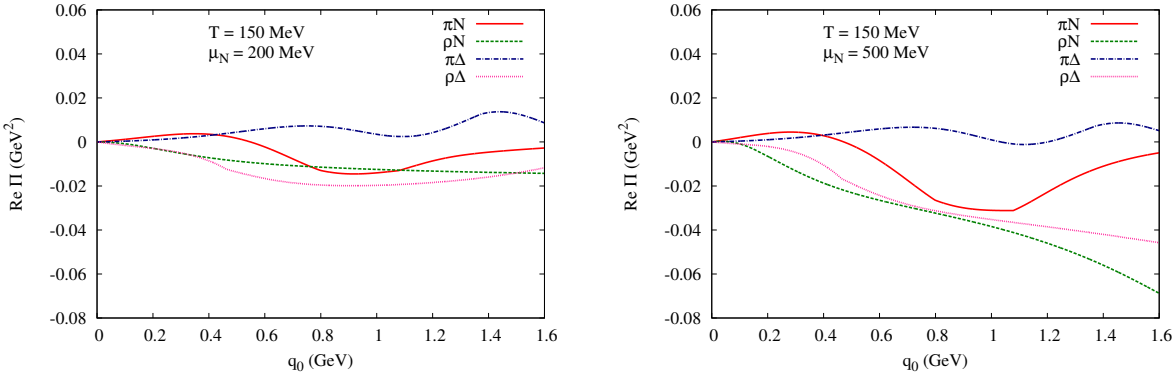

FIG. 6: Same as fig. 5 at T=150 MeV.

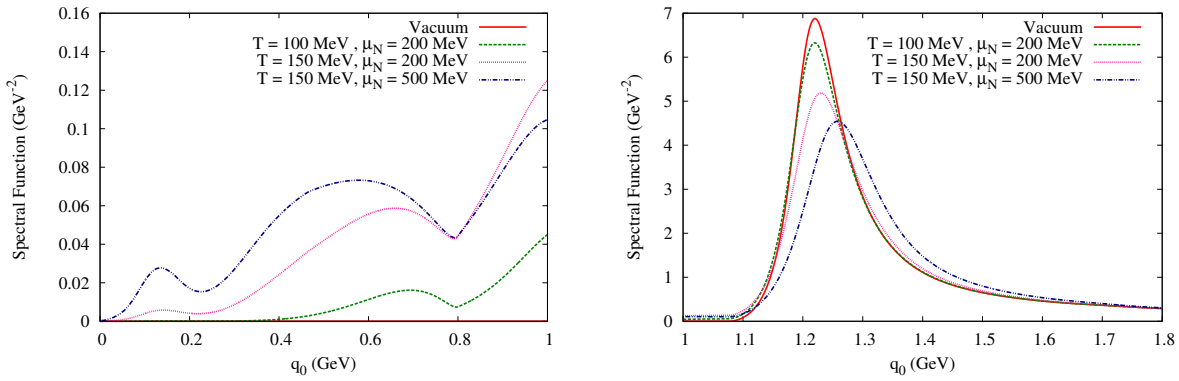
Vacuum
T = 100 MeV , μN = 200 MeV
T = 150 MeV, μN = 200 MeV
T = 150 MeV, μN = 500 MeV
Spectral Function (GeV-2)
q0 (GeV)
Vacuum
T = 100 MeV , μN = 200 MeV
T = 150 MeV, μN = 200 MeV
T = 150 MeV, μN = 500 MeV
Spectral Function (GeV-2)
q0 (GeV)

FIG. 7: The spectral function upto 1 GeV (left) and between 1 to 2 GeV (right)

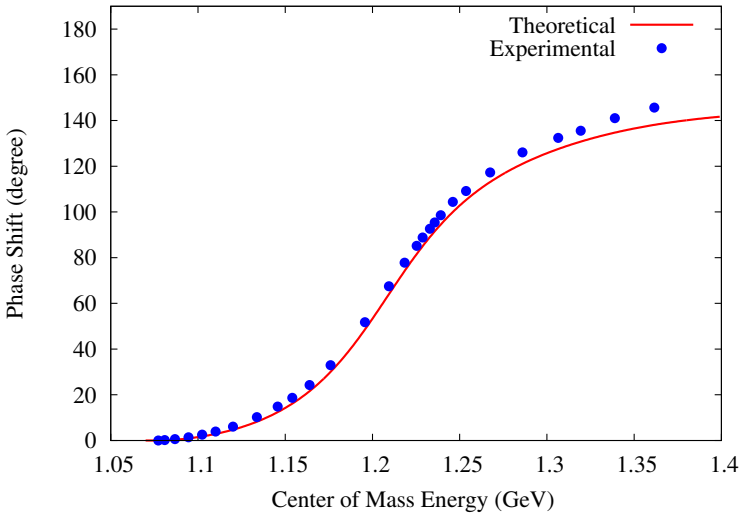

FIG. 8: The πN phase shift compared to data.

spectral density has a significant dependence on the temperature and chemical potential of the medium. There is a gradual suppression of the peak with increasing temperature and density owing to the larger imaginary parts in the denominator of the in-medium propagator.

III. THE π-N CROSS SECTION

Having studied the spectral modification of the Δ in the medium we are now in a position to investigate how these changes affect the πN cross-section. We aim to set up a dynamical framework wherein medium effects can be put in using perturbative methods and which at the same time is normalized to the experimental data in vacuum. We consider the $\pi N\Delta$ interaction (37) and first check with the phase shift data [22] defining $\tan(\delta_{33}) = \frac{\mathrm{Im}f}{\mathrm{Re}f}$ with

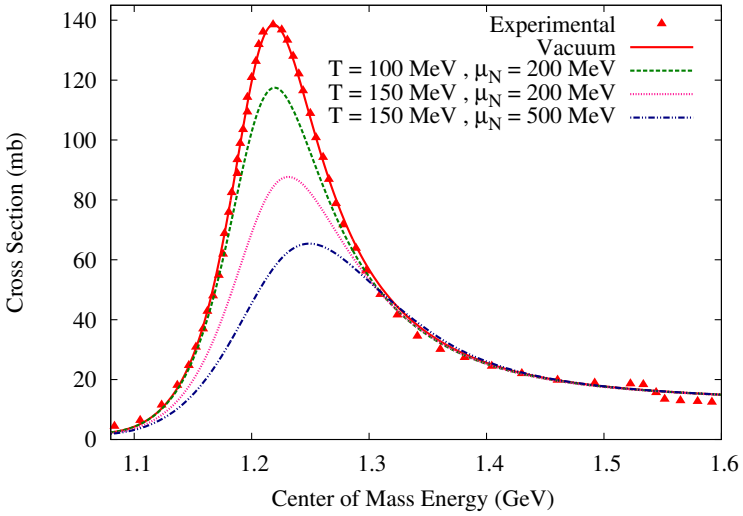

FIG. 9: The π-N scattering cross section with medium effects.

the partial wave amplitude given by $f(E) \sim 1/[E^2 - m_\Delta^2 + i m_\Delta \Gamma(E)]$. The $\Delta \to \pi N$ decay width which follows from the imaginary part of eq. (33) is

$$\Gamma(E) = \frac{1}{24\pi}\left(\frac{f_{\pi N\Delta}}{m_\pi}\right)^2 F^2(E)\frac{\vec{p}^{\,3}}{E^2}[(E+m_N)^2 - m_\pi^2] \tag{22}$$

where the c.m. momentum $\vec{p}^{\,2} = [E^2 - (m_N + m_\pi)^2][E^2 - (m_N - m_\pi)^2]/4E^2$. As seen in fig. 8, a reasonable agreement is obtained using $\Lambda = 600$ and $m_\Delta = 1234$ MeV.

Next we evaluate the matrix elements for elastic πN scattering in the isospin basis in which we replace the free vacuum Δ propagator by an effective one containing the vacuum self energy due to the loop diagrams mentioned above. Averaging over isospin, the squared invariant amplitude for the process $\pi(k)\ N(p) \to\ \pi(k')\ N(p')$ is given by

$$\begin{aligned}
|\bar{\mathcal{M}}|^2 &= \frac{\sum(2I+1)|\mathcal{M}_I|^2}{\sum(2I+1)} \\
&= \frac{1}{3}\left(\frac{f_{\pi N\Delta}}{m_\pi}\right)^4 \left[\frac{F^4(k,p)T_s}{|s - m_\Delta^2 - \Pi|^2} + \frac{F^4(k,p')T_u}{(u-m_\Delta^2)^2}\right. \\
&\qquad \left. + \frac{2F^2(k,p)F^2(k,p')T_m(s - m_\Delta^2 - \mathrm{Re}\Pi)}{3(u-m_\Delta^2)\,|s - m_\Delta^2 - \Pi|^2}\right]
\end{aligned} \tag{23}$$

where T_s, T_u and T_m are given by

$$T_s = \mathrm{Tr}\left[(\not{p}' + m_N) D_s (\not{p} + m_N)\gamma^0 D_u^\dagger \gamma^0\right] \tag{24}$$

$$T_u = \mathrm{Tr}\left[(\not{p}' + m_N) D_u (\not{p} + m_N)\gamma^0 D_u^\dagger \gamma^0\right] \tag{25}$$

$$T_m = \mathrm{Tr}\left[(\not{p}' + m_N) D_s (\not{p} + m_N)\gamma^0 D_u^\dagger \gamma^0\right] \tag{26}$$

in which

$$D_s = k_\alpha k'_\beta \mathcal{O}^{\beta\nu} \Sigma_{\mu\nu}(q_s) \mathcal{O}^{\mu\alpha} \tag{27}$$

$$D_u = k'_\alpha k_\beta \mathcal{O}^{\beta\nu} \Sigma_{\mu\nu}(q_u) \mathcal{O}^{\mu\alpha} \tag{28}$$

where $\Sigma_{\mu\nu}$ is defined in (15).

The cross-section given by $\sigma(s) = \frac{1}{64\pi^2 s} \int |\bar{\mathcal{M}}|^2 d\Omega$ turns out to be in good agreement with the isospin averaged total elastic cross-section given in [23] (obtained using phase shift and inelasticity data from [24] and [22])up to about 1.5 GeV as seen from the solid curve in fig. 9. Having thus normalized the framework with the experimental data we now turn on the medium effects. We replace the vacuum self energy in the above expressions by the in-medium ones evaluated in the real-time formalism described above. A significant suppression of the peak with increasing temperature is obtained accompanied by a small upward shift at higher baryon densities.

IV. SUMMARY AND OUTLOOK

In this work we have studied the medium modification of the Δ baryon properties. The self-energy was evaluated from one-loop graphs comprising of π, ρ, N and Δ using the real-time formulation of thermal field theory. In addition to the contributions from decay processes occurring above thresholds which arise due to the usual thermally weighted unitary cut in the complex q_0 plane there are significant contributions coming from the Landau type discontinuities in the low q_0 region stemming from scattering processes leading to the absorption of Δ in the medium. The πN cross-section is then evaluated with the effective propagator of the Δ leading to a suppression at finite temperature and density with no significant shift of the peak position. This is certain to have non-trivial consequences on the thermalization rate of pions [5] and nucleons produced in heavy ion collisions. In addition, transport properties of such a system is expected to be affected non-trivially.

V. APPENDIX

A. Diagonalising the fermion propagator

The procedure of diagonalization of the thermal matrices appearing in the real time formulation of thermal field theory only concerns the bosonic or fermionic nature of the field [19]. The spin sum which appears in the numerator of the propagator can thus be factored out. The free thermal fermion propagator matrix is written as $\boldsymbol{S}(p) = (\not{p} + m)\boldsymbol{E}(p)$ where the matrix $\boldsymbol{E}$ has components

$$\begin{aligned} E_{11} &= -E_{22}^{*} = \Delta(p,m) - 2\pi i \tilde{N}_1^2 \delta(p^2 - m^2) \\ E_{12} &= -2\pi i e^{\beta\mu/2} \tilde{N}_1 \tilde{N}_2 \delta(p^2 - m^2) \\ E_{21} &= 2\pi i e^{-\beta\mu/2} \tilde{N}_1 \tilde{N}_2 \delta(p^2 - m^2) \ . \end{aligned} \tag{29}$$

The terms $\tilde{N}_1$ and $\tilde{N}_2$ containing thermal factors are given by

$$\begin{aligned} \tilde{N}_1(p_0) &= \sqrt{\tilde{n}_+^p}\,\theta(p_0) + \sqrt{\tilde{n}_-^p}\,\theta(-p_0) \\ \tilde{N}_2(p_0) &= \sqrt{1-\tilde{n}_+^p}\,\theta(p_0) - \sqrt{1-\tilde{n}_-^p}\,\theta(-p_0)\,. \end{aligned} \tag{30}$$

where

$$\tilde{n}_\pm^p = \frac{1}{e^{\beta(\omega_p \mp \mu_p)} + 1} \ , \quad \omega_p = \sqrt{\vec{p}^2 + m^2} \ .$$

The matrix $\boldsymbol{E}$ can be diagonalized as

$$\boldsymbol{E} = \boldsymbol{V} \begin{pmatrix} \Delta & 0 \\ 0 & -\Delta^* \end{pmatrix} \boldsymbol{V} \tag{31}$$

where

$$\boldsymbol{V} = \begin{pmatrix} \tilde{N}_2 & -\tilde{N}_1 e^{\beta\mu/2} \\ \tilde{N}_1 e^{-\beta\mu/2} & \tilde{N}_2 \end{pmatrix} \ . \tag{32}$$

It can be shown [19] that the complete thermal propagator matrix $\boldsymbol{S'}$ is also diagonalized by $\boldsymbol{V}$. From the Dyson equation (7) it then follows that the self energy matrix $\boldsymbol{\Pi}$ is diagonalized by $\boldsymbol{V}^{-1}$ resulting in eq. (8). The diagonal element $\overline{\Pi}$ is given by any one of the four components of $\boldsymbol{\Pi}$. In terms of, say, the 11-component

$$\begin{aligned} \mathrm{Im}\bar{\Pi} &= \epsilon(p_0)\coth[\beta(p_0-\mu)/2]\mathrm{Im}\Pi_{11} \\ \mathrm{Re}\bar{\Pi} &= \mathrm{Re}\Pi_{11} \ . \end{aligned}$$

B. The Δ self-energy in vacuum : Lagrangian and parameters

The Δ self energy in vacuum for the one loop diagrams shown in fig. 1 are given by

$$\Pi^{\mu\nu}_{\pi N} = i\frac{f^2_{\pi N\Delta}}{m^2_\pi}\int\frac{d^4k}{(2\pi)^4}F^2(p,k)\mathcal{O}^{\nu\beta}k_\beta S^0(p)\mathcal{O}^{\alpha\mu}k_\alpha D^0(k) \tag{33}$$

$$\Pi^{\mu\nu}_{\rho N} = i\frac{f^2_{\rho N\Delta}}{m^2_\rho}\int\frac{d^4k}{(2\pi)^4}F^2(p,k)\mathcal{O}^{\nu\eta}\gamma^5\gamma^\phi(g_{\beta\phi}k_\eta - g_{\beta\eta}k_\phi)S^0(p)\gamma^5\gamma^\lambda(g_{\alpha\lambda}k_\sigma - g_{\alpha\sigma}k_\lambda)\mathcal{O}^{\mu\sigma}D_0^{\alpha\beta}(k) \tag{34}$$

$$\Pi^{\mu\nu}_{\pi\Delta} = i\frac{f^2_{\pi\Delta\Delta}}{m^2_\pi}\int\frac{d^4k}{(2\pi)^4}F^2(p,k)\mathcal{O}^{\nu\chi}\gamma^5\gamma^\beta k_\beta\mathcal{O}^{\phi\sigma}g_{\chi\psi}S^0_{\lambda\sigma}(p)\mathcal{O}^{\lambda\eta}\gamma^5\gamma^\alpha k_\alpha\mathcal{O}^{\alpha\mu}g_{\eta\phi}D^0(k) \tag{35}$$

$$\Pi^{\mu\nu}_{\rho\Delta} = if^2_{\rho\Delta\Delta}\int\frac{d^4k}{(2\pi)^4}F^2(p,k)\mathcal{O}^{\nu\chi}(\gamma^\beta + i\frac{\kappa_{\Delta\Delta\rho}}{2m_\Delta}\sigma^{\beta\epsilon}k_\epsilon)\mathcal{O}^{\psi\sigma}g_{\chi\psi}$$
$$S^0_{\lambda\sigma}(p)\mathcal{O}^{\lambda\eta}(\gamma^\alpha - i\frac{\kappa_{\Delta\Delta\rho}}{2m_\Delta}\sigma^{\alpha\delta}k_\delta)\mathcal{O}^{\phi\mu}g_{\eta\phi}D^0_{\alpha\beta}(k) \tag{36}$$

where $D^0(k) = \Delta(k, m_\pi)$ and $D^0_{\mu\nu}(k) = A_{\mu\nu}(k)\Delta(k, m_\rho)$ are the scalar and vector propagators in vacuum. The ones for the spin 1/2 and 3/2 fermions are given by $S^0(p) = (\not{p} + m)\Delta(p, m_N)$ and $S^0_{\mu\nu}(p) = \Sigma_{\mu\nu}(p)\Delta(p, m_\Delta)$ respectively. The vertex factors come from the well-known interactions [25]

$$\mathcal{L}_{\pi N\Delta} = \frac{f_{\pi N\Delta}}{m_\pi}\bar{\Delta}_\alpha\mathcal{O}^{\alpha\mu}\vec{T}^\dagger\partial_\mu\vec{\pi}\psi + H.c. \tag{37}$$

$$\mathcal{L}_{\rho N\Delta} = -i\frac{f_{\rho N\Delta}}{m_\rho}\bar{\Delta}_\alpha\mathcal{O}^{\alpha\mu}\gamma^5\gamma^\nu\vec{T}^\dagger\vec{\rho}_{\mu\nu}\psi + H.c. \tag{38}$$

$$\mathcal{L}_{\pi\Delta\Delta} = \frac{f_{\pi\Delta\Delta}}{m_\pi}\bar{\Delta}^\alpha\mathcal{O}_{\alpha\mu}\gamma^5\gamma^\nu\vec{T}\Delta^\mu\partial_\nu\vec{\pi} \tag{39}$$

$$\mathcal{L}_{\rho\Delta\Delta} = -f_{\rho\Delta\Delta}\bar{\Delta}^\beta\mathcal{O}_{\alpha\beta}\left[\gamma^\mu - \frac{\kappa_{\rho\Delta\Delta}}{2m_\Delta}\sigma^{\mu\nu}\partial_\nu\right]\vec{\rho}_\mu\vec{T}\Delta^\alpha \tag{40}$$

where [12, 25], $f_{\pi N\Delta} = 2.8$, $f_{\rho N\Delta} = 16.03$, $f_{\pi\Delta\Delta} = 1.78$, $f_{\rho\Delta\Delta} = 7.67$ and $\kappa_{\rho\Delta\Delta} = 6.1$. In the above $\mathcal{O}_{\alpha\beta} = g_{\alpha\beta} - a\gamma_\alpha\gamma_\beta$ where the second term contributes only when the spin-3/2 field is off the mass shell. Thus the value of the coupling constants remain unchanged. We take $a = 0.002$ in this work. At each vertex we consider the form factor [26]

$$F(p,k) = \frac{\Lambda^2}{\Lambda^2 + (\frac{p\cdot k}{m_p})^2 - k^2} \tag{41}$$

in which p and k denote the momenta of the fermion and boson respectively.

---

[1] A. Bazavov *et al.*, Phys. Rev. D **85** (2012) 054503

[2] R. Rapp, J. Wambach and H. van Hees, Landolt-Bornstein **23** (2010) 134

[3] S. Sarkar and S. Ghosh, J. Phys. Conf. Ser. **374** (2012) 012010

[4] "The CBM Physics Book," eds. B. Friman et al, Lect. Notes Phys. **814**, 1 (2011).

[5] H. W. Barz, H. Schulz, G. Bertsch and P. Danielewicz, Phys. Lett. B **275** (1992) 19.

[6] S. Mitra, S. Ghosh and S. Sarkar, Phys. Rev. C **85** (2012) 064917

[7] S. Ghosh, S. Sarkar and S. Mallik, Eur. Phys. J. C **70** (2010) 251

[8] S. Mitra and S. Sarkar, Phys. Rev. D **87** (2013) 9, 094026

[9] S. Mitra and S. Sarkar, Phys. Rev. D **89** (2014) 5, 054013

[10] E. Oset and L. L. Salcedo, Nucl. Phys. A **468** (1987) 631.

[11] K. Wehrberger and R. Wittman, Nucl. Phys. A **513** (1990) 603.

[12] C. L. Korpa and A. E. L. Dieperink, Phys. Rev. C **70** (2004) 015207

[13] H. c. Kim, S. Schramm and S. H. Lee, Phys. Rev. C **56** (1997) 1582

[14] L. h. Xia, P. J. Siemens and M. Soyeur, Nucl. Phys. A **578** (1994) 493.

[15] C. L. Korpa and R. Malfliet, Phys. Rev. C **52** (1995) 2756.

[16] H. van Hees and R. Rapp, Phys. Lett. B **606** (2005) 59

[17] E. L. Hjort *et al.*, Phys. Rev. Lett. **79** (1997) 4345.

[18] D. K. Mishra [STAR Collaboration], J. Phys. Conf. Ser. **50** (2006) 315.

[19] S. Mallik and S. Sarkar, Eur. Phys. J. C **61** (2009) 489

[20] M. Le Bellac, *Thermal Field Theory* (Cambridge University Press, Cambridge, 1996).

[21] P. Gonzalez, E. Oset and J. Vijande, Phys. Rev. C **79** (2009) 025209

[22] R. Koch and E. Pietarinen, Nucl. Phys. A **336** (1980) 331.

[23] M. Prakash, M. Prakash, R. Venugopalan and G. Welke, Phys. Rept. **227** (1993) 321.

[24] P. Bareyre, C. Bricman and G. Villet, Phys. Rev. **165** (1968) 1730.

[25] O. Krehl, C. Hanhart, S. Krewald and J. Speth, Phys. Rev. C **62** (2000) 025207

[26] S. Ghosh, S. Sarkar and S. Mallik, Phys. Rev. C **82** (2010) 045202